Article

A competitive-type pressure-dependent immunosensor for highly sensitive detection of Diacetoxyscirpenol in wheat via monoclonal antibody

Xiaoqian Tang, Jing Wu, Wenqin Wu, Zhaowei Zhang, Weiqi Zhang, Qi Zhang, Wen Zhang, Xiaomei Chen, and Peiwu Li

Anal. Chem., **Just Accepted Manuscript** • DOI: 10.1021/acs.analchem.9b03933 • Publication Date (Web): 03 Jan 2020

A competitive-type pressure-dependent immunosensor for highly sensitive detection of Diacetoxyscirpenol in wheat via monoclonal antibody

Xiaoqian Tang [a,#], Jing Wu [a,#], Wenqin Wu[a,#], Zhaowei Zhang [a,*], Weiqi Zhang [a], Qi Zhang[d], Wen Zhang [a,b,c], Xiaomei Chen [a], Peiwu Li [a,b,c,d,e]

[a] Oil Crops Research Institute, Chinese Academy of Agricultural Sciences, Wuhan 430062, China

[b] Key Laboratory of Biology and Genetic Improvement of Oil Crops, Ministry of Agriculture, Wuhan 430062, China

[c] Laboratory of Quality & Safety Risk Assessment for Oilseed Products (Wuhan), Ministry of Agriculture, Wuhan 430062, China

[d] Key Laboratory of Detection for Mycotoxins, Ministry of Agriculture, Wuhan 430062, China

[e] Quality Inspection & Test Center for Oilseed Products, Ministry of Agriculture, Wuhan 430062, China

* Corresponding authors at: Oil Crops Research Institute, Chinese Academy of Agricultural Sciences, Wuhan 430062, P.R.China

Tel.: +86 27 86812862

Fax: +86 27 86812862

E-mail: zwzhang@whu.edu.cn

[#]These authors rank the first authors.

ABSTRACT

Diacetoxyscirpenol (DAS) is a type A trichothecene mycotoxin with low molecular weight, and with respect to its toxicity and the occurrence in food and feed, it is known as a potential risk for public and animal health . In the present study, firstly, a sensitive and specific monoclonal antibody (5E7) was developed. Then, the antibody was applied to develop a competitive-type pressure-dependent immunosensor (CTPDI). The Au@PtNP was synthesized and labeled with goat anti-mouse antibody (Au@PtNPs-IgG). Finally, the concentration of DAS was negatively correlated with the pressure signal. In the presence of optimal conditions, matrix-matched calibration curves were plotted for wheat samples, in which an optimal IC50 value (half maximal inhibitory concentration) of 3.08 ng/g was achieved. The CTPDI was further applied to detect natural and blind wheat samples, and validation was carried out by liquid chromatography-tandem mass spectrometry (LC-MS/MS). The results showed that CTPDI was highly appropriate and accurate for detection of DAS in wheat.

KEYWORDS: Diacetoxyscirpenol; Au@PtNPs; Pressure; Immunosensor; Wheat.

INTRODUCTION

Mycotoxins are secondary metabolites produced by microfungi that are capable of causing disease and death in humans and other animals [1]. Among them, 4,15-Diacetoxyscirpenol (DAS), a secondary metabolite product of the genus Fusarium, is a mycotoxin from the group of type A trichothecenes[2]. The digestion of DAS may induce haematologic disorders (e.g., neutropenia and aplastic anemia)[3], immunosuppression[4], diarrhea, lethargy, and vomiting[5, 6] by inhibiting the synthesis of protein and DNA[7]. DAS has been mainly reported in African, American, and European contries[8-11], while a limited number of cases have been found in Asia. Hence, it is essential to take measures to explore the existence of DAS in wheat, prior to its contamination in food chain.

Several analytical methods were reported to detect DAS, such as liquid chromatography-tandem mass spectrometry (LC-MS/MS)[7], gas chromatography-mass spectrometry (GC-MS)[12,13], and enzyme-linked immunosorbent assay (ELISA)[9]. These methods could facilitate the monitoring of DAS in food products. However, a challenge was noted in developing countries because instruments are costly and skilled operators play a significant role, especially in the on-site monitoring. Quantitative reverse transcription polymerase chain reaction (RT-qPCR) is highly significant to analyze DAS contamination. The development of mouse polyclonal antibodies (pAb), mouse mAbs, and a single chain variable fragment (scFv) antibody were previously reported[15,36]. These antibodies are key reagents for immunoassay, while the accuracy of immunoassay via these antibodies has been found unsatisfactory due to their poor specificity. Performing an ELISA involves at least one antibody with specificity for a particular antigen. The amount of coating antigen is immobilized on a solid support (typically a polystyrene microtiter plate) either non-specifically (via adsorption to the surface) or specifically (via capture by another antibody specific to the same antigen, in a "sandwich" ELISA). After the coating antigen is immobilized, the detection antibody is added, forming a complex with the antigen. Traditional ELISA typically involves chromogenic reporters and substrates

that produce some kinds of observable color changes to indicate the presence of antigen or analyte. The ELISA-like techniques use fluorogenic, electrochemiluminescent, and quantitative PCR reporters to create quantifiable signals. These reporters possess a number of advantages, including higher sensitivities and multiplexing. In technical terms, assays of this type are not strictly ELISAs, as they are not "enzyme-linked", while they are associated with a number of nonenzymatic reporters.[18]

It should be noted that to detect lower concentration, a target amplification technique, typically PCR, is essential. In recent years, with the purpose of, several sensitivity-based detection approaches, including electrochemistry[19], fluorescence[20], colorimetry[21], and surface-enhanced Raman spectroscopy (SERS)[22], have been explored. The employment of transition metal catalyst to produce gases paves a alternative to amplify the signal from antibody-antigen recognition. Compared with traditional ELISA that uses enzyme or fluorescence to produce the signal, two merits can be boasted with this simple manner, including the avoidance of fluorescence background, and significantly increased signal intensity. Consequently, compared with traditional immunoassay, this method allows (1) enhanced sensitivity by an order of magnitude[10]; (2) reduced input-output time to a couple of minutes due to its efficient reaction constant; (3) reliable results by eliminating fluorescence background; (4) an environmental friendly manner by producing only gas[23, 24]. Numerous scholars suggested application of nanoparticles in various fields via generating hydrogen[25], oxygen[26], carbon dioxide[27], etc.. One promising method to produce H_2O_2 on-site is by electrochemical advanced oxidation processes (EAOPs), which showed a significant advantage in detection of gas[28], cancer biomarkers[29], pathogens[30] and enzymatic activity[31]. The synthesis of Pt-based bimetallic nanoparticles as a catalyst has attracted great attention in recent years. Several metallic elements, such as Pd, Au, Ag, Cu, Co, Fe, and Ni have been utilized to synthesize bimetallic nanoparticles with Pt and significant achievements were previously accomplished[32]. Zhu developed simple, rapid, and low cost paper-based

point-of-care testing (POCT) sensors with high sensitivity and portability for disease biomarker detection[33]. Cu^{2+} can catalyze the oxidation of cysteine into cystine by O_2, thereby depressing cysteine-induced aggregation of AuNPs. Based on this method, Yang's group developed a colorimetric immunoassay to determine the cancer biomarker α-fetoprotein[23]. Tang et al. reported a plasmonic ELISA for the quantitative assessment of prostate surface antigen (PSA) based on antibody-labeled GOx-catalyzed oxidation of glucose (Glu) to produce H_2O_2 and the triangular Ag nanoprism[34].

In the present study, we first developed mAbs against DAS from hybridoma cell lines, and synthesized Au@PtNPs before labelling with the second antibody. Then, we fabricated a competitive-type pressure-dependent immunosensor (CTPDI) to detect DAS in wheat. The CTPDI was further validated by LC-MS/MS.

MATERIALS and METHODS

Materials and reagents. DAS was purchased from Toronto Research Chemicals Inc. (Toronto, ON, Canada); Deoxynivalenol (DON), T-2, HT-2, ochratoxin A (OTA, fumonisin B_1 (FB_1), 3-Acetyl DON, ovalbumin (OVA), bovine serum albumin (BSA), 1-(3-Dime-thylaminopropyl)-3-ethylcarbodiimide hydrochloride (EDC), Freund's complete adjuvants (FCA), Freund's incomplete adjuvants (FIA), hypoxanthine-aminopterin-thymidine (HAT), hypoxanthine-thymidine (HT), polyethylene glycol 1500 (PEG 1500, 50%), goat anti-mouse immunoglobulin (IgG), and 3,3',5,5'-tetramethyl benzidine (TMB), chloroplatinic acid hexahydrate ($H_2PtCl_6.6H_2O$), and ammonium acetate (analytical grade) were purchased from Sigma-Aldrich (St. Louis, MO, USA). Clone easy® medium was purchased from Beijing Biodragon Immunotechnologies Co., Ltd. (Beijing, China). Pierce® Rapid ELISA Mouse mAb Isotyping kit, Roswell Park Memorial Institute (RPMI)-1640 medium with l-glutamine, HEPES (free acid, 238.3 g/L), penicillin (+10,000 U/mL), streptomycin (+10,000 μg/mL), as well as methanol and acetonitrile (both HPLC-MS grade) were provided by Thermo Fisher Scientific (Waltham, MA, USA). Fetal bovine serum (FBS) was purchased from Gibco (Billings, MT, USA). H_2O_2 (30%

aqueous solution) was purchased from Suzhou Crystal Clear Chemical Co., Ltd. (Suzhou, China). In addition, 0.01 M phosphate-buffered saline (PBS, pH 7.4) was prepared by addition of 8 g of NaCl, 2.9 g of $Na_2HPO_4 \cdot 12H_2O$, 0.2 g of KH_2PO_4, and 0.2 g of KCl in 1000 mL of deionized water. Water was obtained from a MilliQ purification system (Millipore, Danvers, MA, USA). All reagents were provided by commercial suppliers and used without further purification.

Instrumentation: The absorbance at wavelength of 450 nm was detected using a SpectraMaxM2e microplate reader (Molecular Devices, Sunnyvale, CA, USA). Samples were analyzed by an LCMS-8060 (Shimadzu Corp., Kyoto, Japan). Cell culture plates obtained from Iwaki (Osaka, Japan) were used for hybridoma culture. Polystyrene 96-well microtiter plates were purchased from Costar Co., Ltd. (Costar 3590; Zhengzhou, China). The vacuum freeze dryer was obtained from Thermo Fisher Scientific (Waltham, MA, USA). The statistical analysis was conducted by Origin 8.0 software.

Animals and cells: Female BALB/c mice (age, 6-8 weeks) were purchased from Wuhan Institute of Biological Products Co., Ltd. (Wuhan, China). Besides, SP2/0 myeloma cells were purchased from China Center for Type Culture Collection (CCTCC; Wuhan, China). All animal experiments were performed in accordance with the Beijing Experimental Animal Welfare Ethics Review Guidelines (No 42101200002708).

Synthesis of DAS-hemiglutarate-OVA (BSA). DAS-hemiglutarate-OVA (BSA) was synthesized as described earlier. First, DAS-hemiglutarate (DAS-HG) was synthesized[16]. Briefly, 10 mg DAS (27.2 mmol/L) and 188 mg glutaric anhydride (1.6 mmol/L) were mixed in 5 mL dried tetrahydrofuran with 1 mol/L *N,N*-dimethylpyridin-4-amine (DMAP) as catalyst. The reactions in the mixture were completed at 20 °C overnight. The obtained solvent was evaporated, the residue was dissolved in chloroform, and was subsequently lyophilized. Coupling DAS-HG to bovine serum albumin (BSA) was performed using carbodiimide method. Then, 5 mg of DAS-HG was added to 1 mL methanol dropwise with stirring to a solution,

containing 100 mg 4-ethyl-2,3-dioxo-1-piperazine carbonyl chloride (EDPC, 0.09 mmol/L), mixed with 5 mg BSA (or ovalbumin, OVA) in 2 mL distilled water, and then, the reaction was completed at room temperature overnight. The obtained mixture (DAS-HG-BSA) was subsequently dialyzed against phosphate-buffered saline (PBS) for three days.

Screening of mAb against DAS. Three six-year-old female BALB/c mice were immunized by DAS-HG-BSA (100 μg). After fourth immunization, the serum of mice with the highest titer was used for cell fusion. The positive hybridomas were screened by using a two-step method[35]. The mAb was futher purified from ascites fluid by ammonium sulfate precipitation, and its affinity was evaluated by IC50 value using an indirect competitive ELISA (icELISA). IC50 is the concentration of DAS where the response (signal) is reduced by half. We use origin fit a dose response curve between logarithms of concentration of DAS and signals. Substitute Y=0.5 into the equation, we will got IC50 that the value from X axis.

Synthesis of Au@PtNPs. AuNPs were prepared by using sodium citrate reduction as previously described[35]. The Au@PtNPs were synthesized as follows: 50 mL AuNPs and 1 mL H_2PtCL_6 aqueous solution (3.86 mmol/L) were heated at 85 ˚C for 30 min, and stirred at gentle magnetic. Then, 2 mL of ascorbic acid (10 mmol/L) was added and maintained at 85 ˚C for 30 min. The obtained solution was stored at 4 ˚C.

Preparation of Au@PtNPs-IgG. The goat anti-mouse IgG (4 mg/mL, 20 μL) was added dropwise to 4 mL Au@PtNPs. After incubating for 30 min at 37 ˚C, 0.1% blocking buffer (100 mM $NaHCO_3$, 0.5% casein, 0.25% Tween-20, 5% sucrose, pH 9.0) was added to block the residual sites on Au@PtNPs. After stirring for 2.5 h, the solution was centrifuged twice at 9, 581×g for 10 min to remove the supernatant. The final pellet of Au@PtNPs-IgG was re-suspended in 4 ml stored buffer (10 mM 2-[4-(2-hydroxyethyl) piperazin-1-yl] ethanesulfonic acid, 10 mM citric acid, 0.1% Tween-20, 5% sucrose, pH 7.0).

Electrochemical measurements. Electrochemical measurements were carried out

using a CHI 660E electrochemical workstation (CH Instruments Co., Ltd., Shanghai, China). A conventional three-electrode system was employed as well. The working electrode was made by casting the Au@PtNPs as a thin film onto a glassy carbon rotating disk electrode (RDE, geometrical area = 0.196 cm^2), with Nafion solution as the binding agent. Saturated calomel electrode (SCE) and Pt wire were used as reference electrode and counter electrode, respectively. The assay ink was prepared by adding 1 mL Au@PtNPs aqueous solution to 0.1 mL of 0.05% Nafion solution. 1 mL of fresh assay ink was dropped on the RDE. Potentials are respect to the SHE.

CTPDI for detection of DAS. We utilized a competitive immunosensor and a gas generator to fabricate CTPDI. A CTPDI was fabricated using a pressure meter with a metal probe, microtiter strip, rubber, and a metal case (Scheme 1). The DAS-HG-OVA was immobilized on a microtiter strip, and then, mAbs against DAS were added. After washing with PBST (0.05% Tween-20/PBS, v/v) for three times, Au@PtNPs-IgG was added followed by re-washing with PBST for three times. 30% H_2O_2 (100 μL) was added into the microtiter strip before being sealed with the rubber. The amount of O_2 in the micropores was measured by a portable pressure meter. In order to conduct a negative control to the CTPDI, antibody against aflatoxin B_1 (named 1C11), which was synthesized in our laboratory, was used in lieu of DAS antibody, and other affiliated procedures were the same as before.

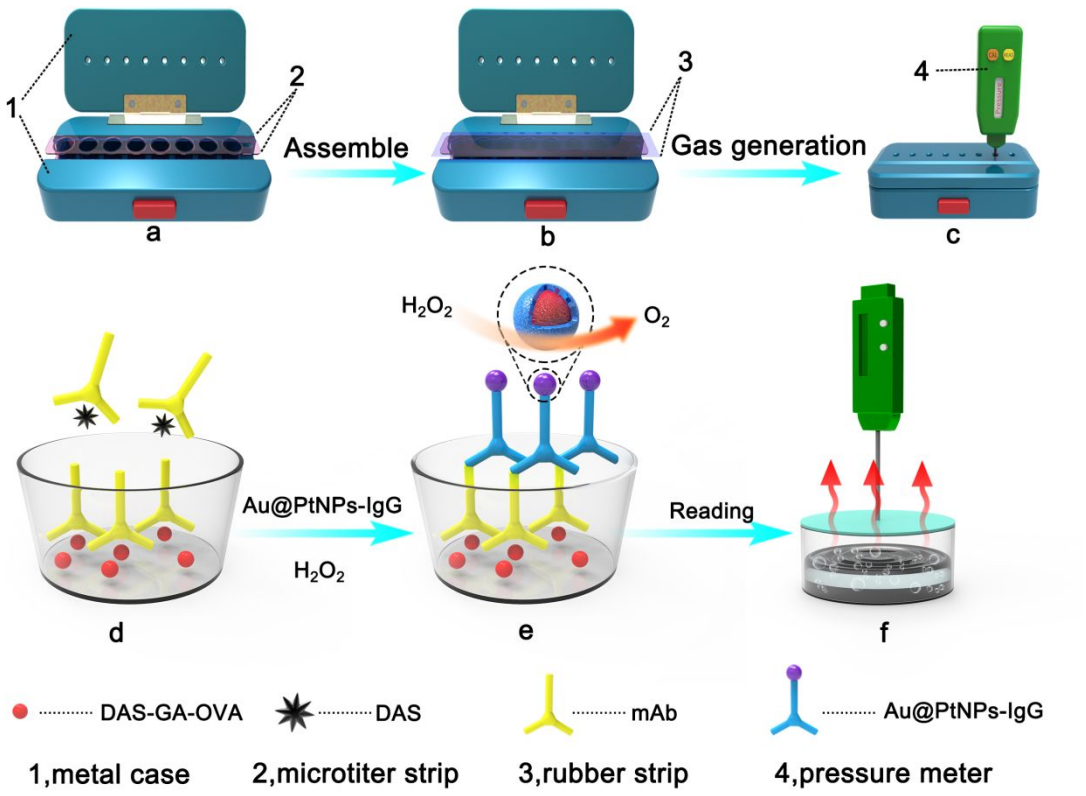

Scheme 1. The schematically illustration of CTPDI for DAS detection. (a) The procedure of putting microtiter strip into the metal case; (b) After addition of 30% H_2O_2 into each micropore of micotiter strip, we put rubber strip on top of micotiter strip; (c, f) Reading P value by a pressure meter; (d) Illustration of competitive immunoreaction. mAb 5E7, which reacted with DAS-HG-OVA, was immobilized in the micropore; (e) Schematically illustration of gas generation

Sample extraction and validation of CTPDI. The extraction of DAS was performed according the following procedure. Here, 10 g of homogenized wheat sample was weighed, then, 40 mL of acetonitrile-water (84:16, v/v) was added, and the mixture was shaken for 10 min. Then, ultra-sonication was carried out for 30 min at 45 ˚C. To purify extracts, 5 mL filtrate was slowly pressed through a 225 Trich Multifunctional column (Romer Labs Inc., Union, MO, USA), and was evaporated to remove the acetonitrile water solution. The residue was reconstituted in 500 μL methanol, in which 400 μL methanol was diluted with 3.6 mL distilled water for analysis of CTPDI, and 100 μL methanol was analyzed by LC-MS/MS.

Spike-and-recovery experiments were evaluated to validate and assess the accuracy of CTPDI. Matrix-matched calibration curves were used at various DAS concentrations (2000, 500, 125, 31.25, 7.81, 1.95, 0.48, and 0.12 ng/mL). The calibration curves were constructed by plotting P_x/P_0 versus concentration of DAS (log 10) using Origin graphic 8.6 software (Origin Lab Corporation, Northampton, MA, USA), and each data point represents the average of three independent measurements.

LC-MS/MS analysis. LC-MS/MS analysis was carried out as previously reported[8]. For this purpose, LC/MS-8060 system equipped with ESI^+ and ESI^- sources (Shimadzu Corp., Kyoto, Japan) was utilized, and the column used was C18 with dimension of 2.1 mm × 50 mm × 1.7 μm. Mobile phase A was 5 mM ammonium formate, and mobile phase B was methanol. The flow rate was 0.3 mL/min, which applied for 0.01-2.50 min, 75-25% A; 2.5-3.0 min, 25-75% A; 3.0-5.5 min, 75-25% A; 5.5-6.0 min, 25-75% A; 6.0-8.0 min, 75-25% A. The total run time was 8 min, and the volume of injection was 20 μL. The column and samples were maintained at 30 ˚C and 4 ˚C, respectively.

RESULTS AND DISCUSSION

Development and characterization of monoclonal antibodies against DAS. The artificial antigen (DAS-HG) was prepared by using HG for introducing a carboxyl group to DAS, in order to provide a basic structure for coupling with large molecules (BSA or OVA), which could fully expose its specific molecular structure after coupling with large molecules (Figure S1). DAS-HG-BSA was used as an immunogen in the immunization procedure. Besides, DAS-HG-OVA was chosen as a coating antigen for detection of positive hybridomas. A total of 256 clones were eventually screened out from the semisolid medium (RPMI1640 medium supplemented with 20% (v/v) FBS, methylcellulose, HAT, antibiotics and HEPES), and the optical density (OD) values were detected with SpectraMaxM2e microplate reader. About 96 positive clones were screened by the icELISA in the first step of screening. The serum of clone 5E7, which exhibited the best sensitivity, was finally selected for production of monoclonal antibody. Sensitive and specific antibodies are

of great significance for achieving reliable and precise results in the antibody-based systems, thus, the characteristics of mAb 5E7 were assessed. The affinity constants of mAbs 5E7 were determined by the icELISA, and the results indicated that high affinity was achieved for DAS ($K = 5.4 \times 10^8$) (Figure S2). Table S1 shows the results of cross-reactivity testing for mAb 5E7 that was detected by ELISA. The interferences with T-2 toxin, HT-2 toxin, DON, 3-acetyl-DON, FB_1, and OTA were almost negligible. Several scholars have already reported development of DAS antibodies. The monoclonal antibodies reported by Klaffer et al.[36] and PAULY et al.[37] exhibited cross-reaction with T-2. However, in the present study, mAb 5E7 had no cross-reaction with T-2 toxin, HT-2 toxin, DON, 3-acetyl-DON, FB_1, and OTA.

Characterization of Au@PtNPs and Au@PtNPs–IgG. We, in the present study, conducted transmission electron microscopy (TEM) to determine the size and shape of Au@PtNPs. The TEM images and corresponding photo images (Figure 1a, b) showed that the Au@PtNPs and Au@PtNPs–IgG tended to be uniformly distributed. The Au@PtNPs were 15 nm in size, with a rounded circular appearance (Figure 1c, d). Figure 1e-h shows that Au was located in the core of the NPs, whereas Pt was located on the surface of Au. The nanostructures of Au@PtNPs were analyzed by the X-ray powder diffraction (XRD), and the peak values of Au@PtNPs were recorded at 38.4°, 45.6°, 66.4°. Comparing Au@PtNPs with Au, Pt alone showed that the diffraction peak position of Au@PtNPs was between the individual Au (38.2°, 44.3°, 64.6°, 77.6°, 81.7°)[38] and Pt (40.1°, 46.6°, 68.1°)[39]. It also was noted that width of the diffraction peak for Au@PtNPs was not a simple superposition of Au and Pt, which indicated that Au@PtNPs could be found as alloy rather than a physical mixture of both. The optical properties of Au@PtNPs and Au@PtNPs-IgG were identified by ultraviolet–visible spectroscopy (UV-vis). As illustrated in Figure 2b, a small peak at around 280 nm for the Au@PtNPs-IgG could be attributed to the unique absorption of IgG, indicating that IgG was labeled on the nanoparticles[30]. The Au@PtNPs-IgG was also evidenced by comparing the energy-dispersive X-ray spectroscopy (EDS) of Au@PtNPs before and after conjugation, as shown in Figure 2c, d. Characteristic

peaks of C and N images were remarkably higher in the spectrogram of Au@PtNPs after being conjugated with antibodies, demonstrating that Au@PtNPs and IgG were successfully conjugated. The relative coupling rate (RCE) was assessed to calculate the rate of modified IgG on the Au@PtNPs, which was formulated as follows,

$$\text{RCE (μg/mg)} = \frac{M_1 - M_2}{M_{\text{Au@PtNPs}}} \quad [1]$$

where M_1 represents the original amount of added IgG, M_2 denotes the residual amount of IgG in the supernatant, and $M_{\text{Au@PtNPs}}$ is the amount of Au@PtNPs. The results indicated that the RCE value was 7.5 μg/mg. The Au@PtNPs solution exhibited a Zetasize with 37.8 nm and a negative zeta potential value of -47.6, which illustrated high stability of the Au@PtNPs solution. After conjugated with IgG, Zetasize was 21 nm, with a negative zeta potential value of -26.2, indicating a successful production of Eu(III) nanoparticle-labeled mAbs.

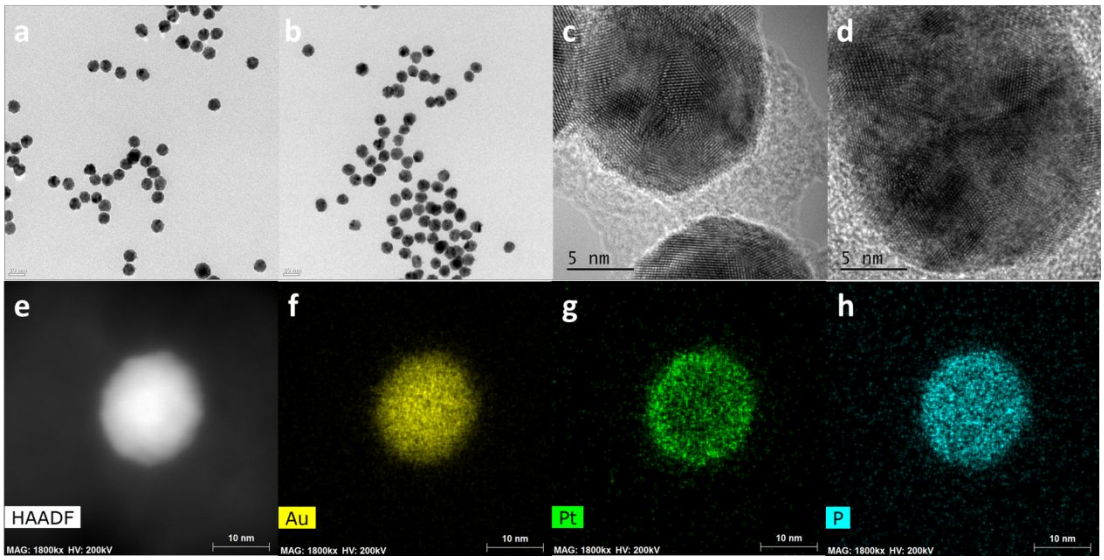

Figure 1. TEM images of Au@PtNPs (a, c) and Au@PtNPs-IgG (b, d); TEM-mapping obtained for Au@PtNPs (e); Illustration of Au, which was located in the core of the NPs (f); Illustration of Pt, which was located on the surface of Au (g); Image of P (h).

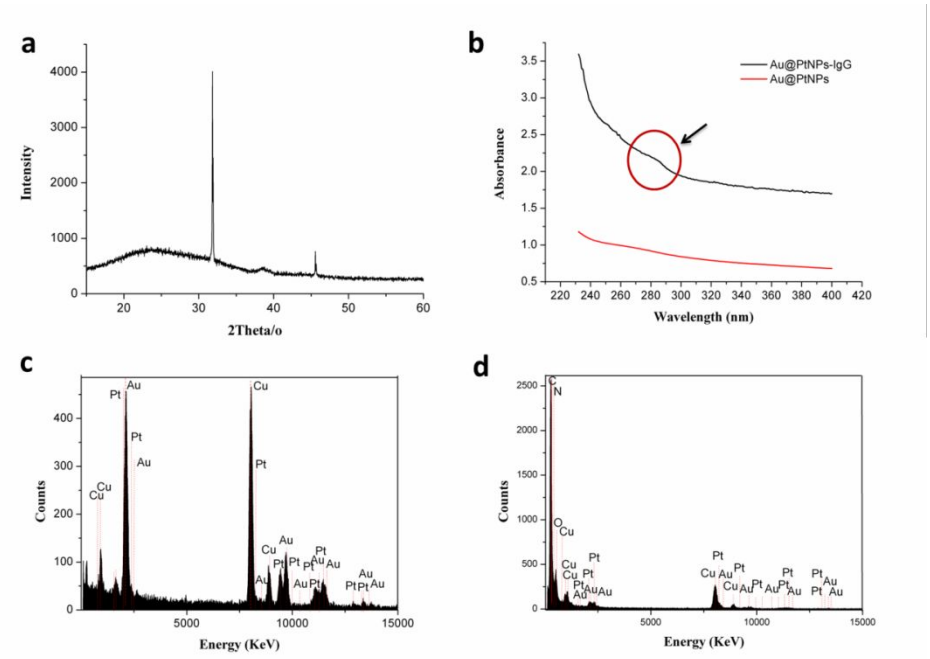

Figure 2. X-ray images were obtained from Au@PtNPs (a); UV-vis of Au@PtNPs and Au@PtNPs-IgG (b); EDS of Au@PtNPs (c); EDS of Au@PtNPs-IgG (d).

Electrochemical measurements. In order to confirm the generation of O_2, the Au@PtNPs were tested for their oxygen reduction reaction (ORR) in a sealed glass cell using a three-electrode system in 0.5 M H_2SO_4 at 25 ^oC in presence of H_2O_2. The measurements were carried out using a rotating disk electrode (RDE, geometrical area = 0.196 cm^2) by linear sweep voltammetry (LSV) at 5 mV s^{-1}, at rotation speeds of 1800 rpm.

The performances of experiments were compared. Firstly, the ORR performance of the Au@PtNPs modified RDE in the pure nitrogen saturated 0.5 M H_2SO_4 solution was investigated, in which the corresponding LSV curve was shown in Figure 3a, and no remarkable ORR was observed in 0.5 M H_2SO_4 solution in absence of H_2O_2. Secondly, the electrolyte was deoxidized by nitrogen and then H_2O_2 was added; the H_2O_2 was reacted with the Au@PtNPs for 10 min in dark conditions, and then, the ORR was measured. As illustrated in Figure 3b, a notable ORR can be observed in presence of O_2, indicating generation of O_2. The ORR rates of Au@PtNPs were consistent with those reported in previous studies[42-43].

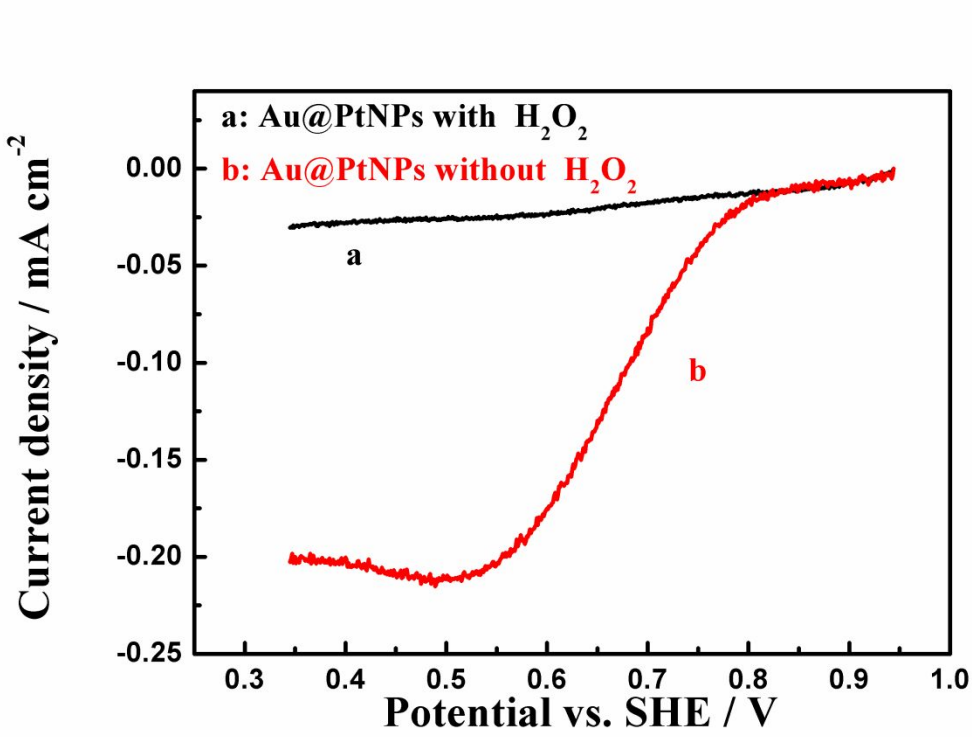

Figure 3. LSVs of oxygen reduction on the Au@PtNPs assay modified RDE in 0.5 M H_2SO_4 presence and absence of hydrogen peroxide at room temperature. Sweep rate: 5 mV s^{-1}. Rotation speed: 1800 rpm.

Analytical performance of the CTPDI. In the present study, Au@PtNPs were synthesized and labeled with IgG. Besides, Au@PtNPs-IgG was used to generate O_2 as an indicator. The O_2 generated in a sealed micropore was detected using a pressure gauge and then was converted into a digitized signal. The pressure values were recoded as P (kPa). Before gas generation, a competitive immunoassay was performed. In detection of positive sample, the free DAS in the sample was combined with the mAb 5E7, then the DAS-mAb 5E7 complex was washed with PBST, so that less or none mAb 5E7 were combined with the DAS-HG-OVA in the micropores, which resulted in less or none Au@PtNPs-IgG captured with the 5E7 in the micropores. The P_x (kPa) values were recorded by a portable pressure meter. In contrast, in detection of negative sample, the mAb 5E7 added into the micropores was combined with the DAS-HG-OVA. The exceeded mAb 5E7 was washed with PBST. After reading pressure gauge, the P values were recorded as P_0 (kPa). The P (kPa) in

each micropore was directly related to the concentration of DAS in the sample. When there is a higher concentration of DAS in the micropore, the DAS consums DAS antibodies, leading to less Au@PtNPs-IgG binding with the antigen in the micropore, and the volume of O_2 deceasing with the amounts of Au@PtNPs-IgG. Therefore, the higher concentration of DAS is directly associated with the lower P (kPa). A control experiment which using 1C11 instead of 5E7 was performed. Assay with 5E7, the P (kpa) values decreasing with DAS concentration increase from 0.12 ng/mL to 2000 ng/mL, while the assay with 1C11 almost obtained none P (kpa) signals (Figure S3).

Optimization of the CTPDI. Several parameters may impact the CTPDI, including blocking buffer, amounts of IgG for Au@PtNPs–IgG conjugation, concentrations of DAS-HG-OVA and mAb 5E7, amounts of Au@PtNPs–IgG, incubation period, and volume of standard solution, in which their influences on CTPDI were assessed. The blocking buffer used in Au@PtNPs–IgG could significantly affect the results of immunoassay. Three kinds of blocking buffer, 0.25% OVA-PBS (w/v), 0.25% nonfat milk-PBS (w/v), and 0.25% casein-PBS (w/v), were investigated. A proper linear correlation was found between the P/P0 ratio and the DAS concentration when the 0.25% casein-PBS (w/v) was used. Different amounts of IgG (2, 4, 8, and 16 μg) labeled with Au@PtNPs were assessed according to the sensitivity of the immunoassay. The results showed that the IC50 was 0.60 ng/mL when the IgG was labeled with 8 μg of Au@PtNPs. The sensitivity was higher in case of labeling with the other concentrations of IgG (0.73-0.94 ng/mL). Eventually, we selected 8 μg as optimum amount of IgG (Figure 4a).

The concentration of coating antigen (DAS-HG-OVA) and the amount of mAb (5E7) added into the micropores were herein optimized. The sensitivity was improved by appropriate reduction of the concentration of antigen. Under various antigen amounts ranging from 8 to 2 μg/mL, the sensitivity increased (Figure 4b). Thus, 2 μg/mL of antigen was here chosen. The amounts of Au@PtNPs-IgG could affect the amounts of gas generation, which was optimized by dispensing Au@PtNPs-IgG with different dilution rates. The results showed that at 10-fold dilution, the sensitivity was higher

(Figure 4c). Additionally, as gas generation between H_2O_2 and the Au@PtNPs-IgG was time-dependent, the effects of various time points on gas generation were assessed, in which a remarkable uncertainty was observed during 5, 10, and 15 min of gas generation, respectively. Therefore, 20 min was found to be associated with high reproducibility and sensitivity, which was chosen for subsequent experiments (Figure 4d). The standard volume of DAS was studied as well; when 25 µL of DAS was added into the well, the final IC50 value was 4-fold higher than using 50 and 100 µL. However, the volume of 50 µL was used in the present experiment because of its higher sensitivity and saving the amounts of chemical reagents (Figure 4e). Different concentrations of methanol applied on a standard curve were studied. The IC50 value was become higher with increasing the concentration of methanol. This indicated that the methanol has a remarkable influence on the reaction of antigen-antibody. As a result, the 10% methanol was therefore chosen for the analysis (Figure 4f).

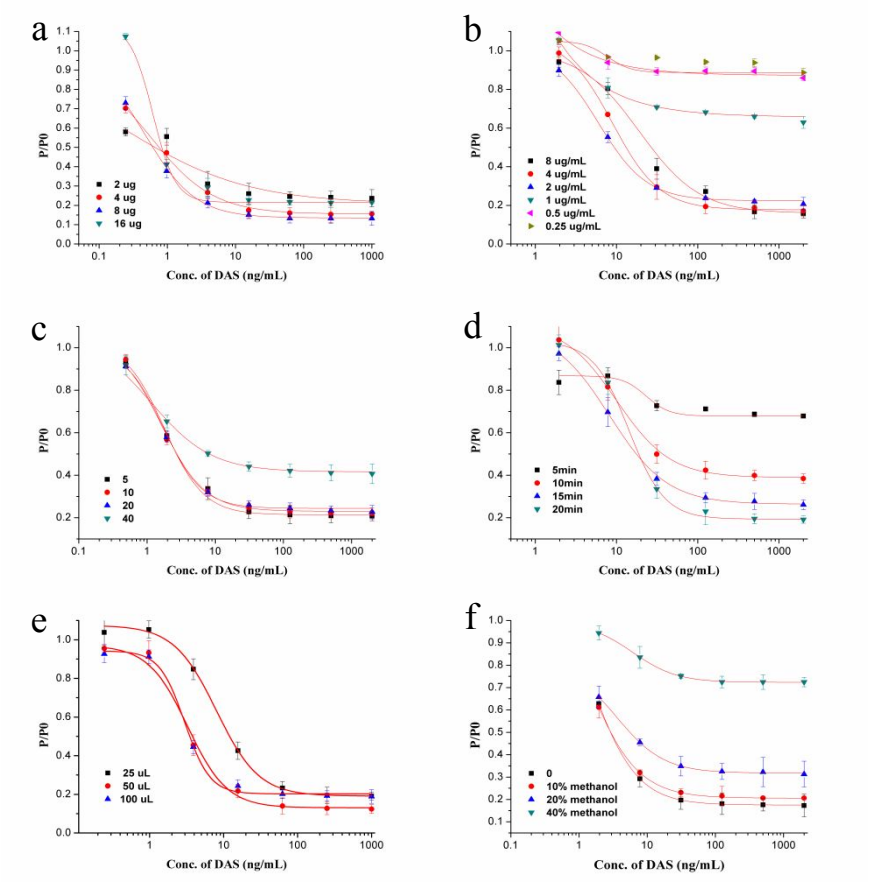

Figure 4. Effects of several factors on standard curves, such as amounts of IgG used in Au@PtNPs-IgG conjugation (a); dilution rates of antibodies (b); dilution rate of Au@PtNPs-IgG (c); incubation period (d) ; volume of DAS standard solution (e); and concentration of methanol (f). The results were expressed as the mean values of three independent experiments.

Specificity of CTPDI assay. DAS is a type A trichothecene mycotoxin produced by some Fusarium species including F. equiseti, F. poae and F. sporotrichioides. It has been reported that Type A trichothecenes, e.g. DAS and T-2 toxin, are generally more cytotoxic than Type B trichothecenes, such as DON. The structure of type B trichothecenes is characterized by a carbonyl group in C8 position, while one of type A trichothecenes has no carbonyl group. The structure of DAS is quite similar with the other trichothecenes, especially with T-2 and HT-2 toxins. We investigated six structurally related mycotoxins, including T-2, HT-2, DON, 3-acetyl-DON, FB_1, and OTA using the CTPDI. As shown in Figure 5a, in different concentrations of mycotoxins (2000, 500, 125, 31.25, 7.81, 1.95, 0.48, and 0.12 ng/mL), DAS caused a reduction in regularity, while the other six structurally related mycotoxins caused almost no changes in P values. The percentage of analytical specificity was calculated as follows: analytical specificity (%) = IC50 (DAS)/IC50 (other toxins) × 100. The corresponding values for DON, FB_1, T-2, HT-2, OTA, and 3-acetyl-DON were 0. Additionally, when compared with previous literatures[36-37], the ELISA based antibodies exhibited cross-reaction with T-2. However, in the present study, CTPDI based mAb 5E7 had no cross-reaction with T-2 toxin, HT-2 toxin, DON, 3-acetyl-DON, FB_1, and OTA which exhited better specificity. Thus, the proposed CTPDI markedly enhanced specificity in DAS detection.

Validation of CTPDI. To validate the CTPDI capability, wheat matrix was employed. DAS is slightly soluble in water and can be dissolved in methanol, ethanol, and acetonitrile. Methanol is a common organic reagent, which could be used in immunoassay[40, 41]. Based on the optimum values of investigated factors, a linear equation was formulated as follows, $y = 0.06+0.083/(1+x/x_0)^{0.7}$, R^2 (correlation

coefficient)= 0.983. The IC50 concentration for the standard curve was 3.08 ng/g, while the linear range caculated by 20% - 80% inhibition is 0.46 - 30.6 ng/g, respectively (Figure 5b). We examined the performance of the CTPDI at different concentrations of DAS (1, 5, 50 ng/mL), the recoveries of the assays were 84.4% - 106.0 %. To study the stability of CTPDI, the intra-assay variation was calculated by the average of six replicated micropores in one microstrip. The inter-assay variation was calculated by the average of six replicated microstrips at different time points. The range of relative standard deviation (RSD) was 7.2%-10.4% for intra-assays and 9.0%-12.1% for inter-assays (Table 1), which indicated the feasibility of determining DAS using CTPDI.

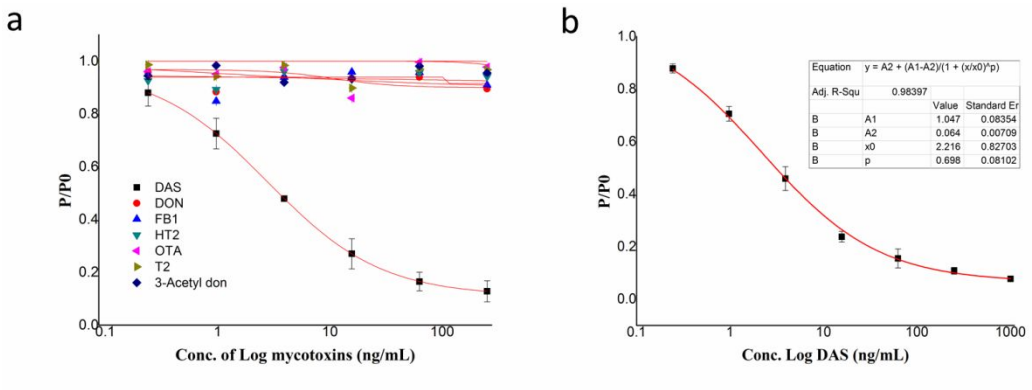

Figure 5. Specificity of CTPDI for detecting DAS (a); The DAS calibration curve for wheat with 2 μg/mL DAS-HG-OVA, 10% methanol, Au@PtNPs-IgG with 10-fold dilution, and gas generation for 20 min (b).

Table 1. Recovery analysis of CTPDI for DAS in wheat samples

	Spiked concentration (ng/mL)	Mean±SD (ng/mL)	Recovery (%)	RSD (%)
Intraday	1.0	1.043±0.8	104.3	10.4
	5.0	4.73±0.91	94.6	7.2
	50.0	43.1±0.37	86.2	8. 0
Interday (n=11)	1.0	1.06±0.5	106.0	12.1
	5.0	4.22±0.80	84.4	10.5
	50.0	45.8±0.6	91.6	9.0

Furthermore, we used CTPDI to detect DAS in ten naturally contaminated wheat

samples, which were collected from different farms. The results were validated by LC-MS/MS. The MS parameters were concluded in Table S2. Well-resolved peaks and good peak shape were achieved for DAS. The results obtained from LC-MS/MS analysis of wheat samples are summarized in Table 2. A total of 7 samples (70% of 10 samples) were found to contain DAS with the concentration of lower than 0.82 ng/g. The findings indicated a satisfactory agreement between the two analytical methods, indicating that the proposed method is highly appropriate for screening and quantitation of DAS in wheat.

Table 2. Validation of the CTPDI by LC-MS/MS

for detecting DAS in ten naturally wheat samples

Sample	HPLC-MS/MS (n=5)	CTPDI (n=5)
	Mean (ng/g)	Mean (ng/g)
1	0.82±0.001	0.75±0.89
2	0.70±0.002	0.65±0.75
3	0.68±0.033	0.64±0.84
4	0.66±0.004	0.62±0.68
5	0.68±0.010	0.67±0.65
6	0.68±0.004	0.60±0.56
7	ND[a]	ND
8	ND	ND
9	0.62±0.058	0.59±0.63
10	ND	ND

[a]ND: not detected

CONCLUSIONS

In summary, a sensitive monoclonal antibody was developed, based on the mAbs, and Au@PtNPs-lgG was synthesized and applied for identification of DAS by CTPDI. Due to specific DAS mAb and excellent biocompatibility of Au@PtNPs-lgG, the proposed CTPDI exhibited an excellent analytical performance with a wide linear

range (0.46-30.6 ng/g), as well as a low IC50 value (3.08 ng/g). In addition, CTPDI showed high repeatability and accuracy, and the ranges of RSD for intra-assays and inter-assays were 7.2%-10.4% and 9.0-12.1%, respectively. The CTPDI was used to detect DAS in wheat samples that accompanied by satisfactory results, and the results were herein validated by LC-MS/MS. Regarding the advantages of high sensitivity, fast detection, low-cost, and on-site, the developed method could be used in detection of hazardous macromolecules.

ASSOCIATED CONTENT

The Supporting Information is available free of charge on the ACS Publications website at DOI:??. Details of additional information show in two tables and three figures.

AUTHOR INFORMATION

Corresponding Authors

*E-mail: zwzhang@whu.edu.cn

ORCID:

Zhaowei Zhang: 0000-0002-6686-2995

Conflict of interest

The authors declare no conflict of interest.

ACKNOWLEDGEMENTS

We appreciate the financial supports by National Key Research and Development Program (2018YFE0206000), Agricultural Science and Technology Innovation Program of CAAS (CAAS-XTCX2019024), and National Natural Science Foundation of China (31601573)

REFERENCES

1. Hao, N.; Lu, J.; Zhou, Z.; Hua, R.; Wang, K., A pH-Resolved Colorimetric Biosensor for Simultaneous Multiple Target Detection. *ACS Sensors* **2018,** *3* (10), 2159-2165.

2. García-Moraleja, A.; Font, G.; Mañes, J.; Ferrer, E., Simultaneous determination of mycotoxin in commercial coffee. *Food Control* **2015,** *57*, 282-292.

3. Thanakarn Nasri, R. R. B., Sandra ten Voorde, Johanna Fink-Gremmels Differential induction of apoptosis by type A and B trichothecenes in Jurkat T-lymphocytes. *Toxicol In Vitro.* **2006,** *20* (6), 832-840.

4. A.M. Ayral, N. D., J. Le Bars & L. Escoula, In vitro effect of diacetoxyscirpenol and deoxynivalenol on microbicidal. *Mycopathologia* **1992,** *120*, 121-127.

5. Bottex, C. M., A.; Fontanges, R., Action of a mycotoxin (diacetoxyscirpenol) on the immune response of the mouse-interaction with an immunomodulator (OM-89). *Immunopharmacol. Immunotoxicol.* **1990,** *12*, 311–325.

6. Chi, M. R., T.; Mirocha, C.; Reddy, K., Acute toxicity of 12, 13-epoxytrichothecenes in one-day-old broiler chicks. *Appl. Environ. Microbiol.* **1978,** *35*, 636–640.

7. Hassanane, M. S., Abdalla, E. S. A., Ei-Fiky, S., Amer, M. A., & Hamdy, A., Mutagenicity of the Mycotoxin diacetoxyscirpenol on somatic and germ cells of mice. *Mycotoxin Res* **2000,** *16* (1), 53-64.

8. Njumbe Ediage, E.; Van Poucke, C.; De Saeger, S., A multi-analyte LC-MS/MS method for the analysis of 23 mycotoxins in different sorghum varieties: the forgotten sample matrix. *Food Chem X* **2015,** *177*, 397-404.

9. Aniołowska, M.; Steininger, M., Determination of trichothecenes and zearalenone in different corn (Zea mays) cultivars for human consumption in Poland. *J Food Compost Anal* **2014,** *33* (1), 14-19.

10. Schollenberger, M.; Muller, H. M.; Ernst, K.; Sondermann, S.; Liebscher, M.; Schlecker, C.; Wischer, G.; Drochner, W.; Hartung, K.; Piepho, H. P., Occurrence and distribution of 13 trichothecene toxins in naturally contaminated maize plants in Germany. *Toxins* **2012,** *4* (10), 778-87.

11. WHO *Technical Report Series*; Geneva, Switzerland, 2017; pp 40-54.

12. Pereira, V. L.; Fernandes, J. O.; Cunha, S. C., Comparative assessment of three cleanup procedures after QuEChERS extraction for determination of trichothecenes (type A and type B) in processed cereal-based baby foods by GC-MS. *Food Chem X* **2015,** *182*, 143-9.

13. Rodriguez-Carrasco, Y.; Ruiz, M. J.; Font, G.; Berrada, H., Exposure estimates to Fusarium mycotoxins through cereals intake. *Chemosphere* **2013,** *93* (10), 2297-303.

14. Schubring S.L.; Chu, F. S., An indirect enzyme-linked immunosorbent assay for the detection of diacetoxyscirpenol in wheat and corn. *Mycotoxin Res* **1987,** *3*, 97-106.

15. Doyle, P. J.; Arbabi-Ghahroudi, M.; Gaudette, N.; Furzer, G.; Savard, M. E.; Gleddie, S.; McLean, M. D.; Mackenzie, C. R.; Hall, J. C., Cloning, expression, and characterization of a single-domain antibody fragment with affinity for 15-acetyl-deoxynivalenol. *Mol Immunol* **2008,** *45* (14), 3703-13.

16. E. N. Clare Mills, J. M. J., Heather A. Kemp and Michael R. A. Morgan, An Enzyme-linkedImmunosorbentAssay for Diacetoxyscirpenol Applied to the Analysis of Wheat. *J Sci Food Agric* **1988,** *42*, 225-233.

17. Pang, P.; Teng, X.; Chen, M.; Zhang, Y.; Wang, H.; Yang, C.; Yang, W.; Barrow, C. J., Ultrasensitive enzyme-free electrochemical immunosensor for microcystin-LR using molybdenum disulfide/gold nanoclusters nanocomposites as platform and Au@Pt core-shell nanoparticles as signal enhancer. *Sens Actuators B Chem* **2018,** *266*, 400-407.

18. Giljohann, D. A.; Mirkin, C. A., Drivers of biodiagnostic development. *Nature* **2009,** *462* (7272), 461-4.

19. Zhang, W.; Dixon, M. B.; Saint, C.; Teng, K. S.; Furumai, H., Electrochemical Biosensing of Algal Toxins in Water: The Current State-of-the-Art. *ACS Sensors* **2018,** *3* (7), 1233-1245.

20. Tagit, O.; Hildebrandt, N., Fluorescence Sensing of Circulating Diagnostic Biomarkers Using Molecular Probes and Nanoparticles. *ACS Sensors* **2016,** *2* (1), 31-45.

21. Zhong, Y.; Chen, Y.; Yao, L.; Zhao, D.; Zheng, L.; Liu, G.; Ye, Y.; Chen, W., Gold nanoparticles based lateral flow immunoassay with largely amplified sensitivity for rapid melamine screening. *Microchimica Acta* **2016,** *183* (6), 1989-1994.

22. Li, J.; Yan, H.; Tan, X.; Lu, Z.; Han, H., Cauliflower-Inspired 3D SERS Substrate for Multiple Mycotoxins Detection. *Anal Chem* **2019**.

23. Liu, D.; Li, X.; Zhou, J.; Liu, S.; Tian, T.; Song, Y.; Zhu, Z.; Zhou, L.; Ji, T.; Yang, C., A fully integrated distance readout ELISA-Chip for point-of-care testing with sample-in-answer-out capability. *Biosens Bioelectron* **2017,** *96*, 332-338.

24. Zhi, Z.; Zhichao, G.; Dan, L.; Shasha, J.; Jiuxing, L.; Zhichao, L.; Shuichao, L.; Tianhai, J.; Zhongqun, T.; and Chaoyong James, Y.*, Translating Molecular Recognition into a Pressure Signal to enable Rapid, Sensitive, and Portable Biomedical Analysis. *Angew Chemint Edit* **2015,** *54*, 10448-10453.

25. Ji, Y.; Yang, L.; Ren, X.; Cui, G.; Xiong, X.; Sun, X., Nanoporous CoP3 Nanowire Array: Acid Etching Preparation and Application as a Highly Active Electrocatalyst for the Hydrogen Evolution Reaction in Alkaline Solution. *ACS Sustain Chem Eng* **2018,** *6* (9), 11186-11189.

26. Xiong, X.; You, C.; Liu, Z.; Asiri, A. M.; Sun, X., Co-Doped CuO Nanoarray: An Efficient Oxygen Evolution Reaction Electrocatalyst with Enhanced Activity. *ACS Sustain Chem Eng* **2018,** *6* (3), 2883-2887.

27. Shin-Ichi, O.; Kyosuke, K.; Toru, M.; Shuta, M.; Masanobu, M.; and Kei, T., Universal HPLC Detector for Hydrophilic Organic Compounds by Means of Total Organic Carbon Detection. *Anal Chem* **2018,** *90* (11), 6461–6467.

28. Zhao, Y.; Yang, Y.; Cui, L.; Zheng, F.; Song, Q., Electroactive Au@Ag nanoparticles driven electrochemical sensor for endogenous H_2S detection. *Biosens Bioelectron* **2018,** *117*, 53-59.

29. Lv, H.; Li, Y.; Zhang, X.; Gao, Z.; Zhang, C.; Zhang, S.; Dong, Y., Enhanced peroxidase-like properties of Au@Pt DNs/NG/$Cu^{(2+)}$ and application of sandwich-type electrochemical immunosensor for highly sensitive detection of CEA. *Biosens Bioelectron* **2018,** *112*, 1-7.

30. Wei, X.; Zhou, W.; Sanjay, S. T.; Zhang, J.; Jin, Q.; Xu, F.; Dominguez, D. C.;

Li, X., Multiplexed Instrument-Free Bar-Chart SpinChip Integrated with Nanoparticle-Mediated Magnetic Aptasensors for Visual Quantitative Detection of Multiple Pathogens. *Anal Chem* **2018,** *90* (16), 9888-9896.

31. Xu, G.; Zhou, H.; Reboud, J.; Cooper, J. M., Cycling of Rational Hybridization Chain Reaction To Enable Enzyme-Free DNA-Based Clinical Diagnosis. *Acs Nano* **2018,** *12* (7), 7213-7219.

32. Lin, C.; Yi-Hsuan, L.; Balamurugan, A.; Vittal, R.; Lin, W.; Ho C., Electrode modified with a composite film of ZnO nanorods and Ag nanoparticles as a sensor for hydrogen peroxide. *Talanta* **2010,** *82*, 340–347.

33. Yi, X.; Xiaofeng, W.; Qizhen, Y.; Zhichao, G.; Dan, L.; Xuan, L.; Leiji, Z.; Zhi, Z.; Zhenyu, L.; Chaoyong, Y., A Shake&Read distance-based microfluidic chip as a portable quantitative readout device for highly sensitive point-of-care testing. *Chem Commun* **2016,** *52*, 13377.

34. Yu, Z.; Tang, Y.; Cai, G.; Ren, R.; Tang, D., Paper Electrode-Based Flexible Pressure Sensor for Point-of-Care Immunoassay with Digital Multimeter. *Anal Chem* **2018,** *91*, 1222−1226.

35. Zhang, D.; Li, P.; Zhang, Q.; Zhang, W., Ultrasensitive nanogold probe-based immunochromatographic assay for simultaneous detection of total aflatoxins in peanuts. *Biosens Bioelectron* **2011,** *26* (6), 2877-82.

36. Klaffer, U.; Märtlbauer, E.; Terplan, G., Development of a sensitive enzyme-linked immunosorbent assay for the detection of diacetoxyscirpenol. *Int J Food Microbiol* **1988,** *6*, 9-17.

37. PAULY, J.U.; Bitter-Suermann D.; Dose, K., Production and Characterization of a Monoclonal Antibody to the Trichothecene Mycotoxin Diacetoxyscirpenol. *Biol. Chem. Hoppe-Seyler* **1988,** *369*, 487-492.

38. Cuevas-Muñiz, F. M.; Guerra-Balcázar, M.; Castaneda, F.; Ledesma-García, J.; Arriaga, L. G., Performance of Au and AuAg nanoparticles supported on Vulcan in a glucose laminar membraneless microfuel cell. *J Power Sources* **2011,** *196* (14), 5853-5857.

39. Hassan, H. K.; Atta, N. F.; Galal, A., Electrodeposited nanostructured Pt–Ru

co-catalyst on graphene for the electrocatalytic oxidation of formaldehyde. *J Solid State Electrochem* **2013,** *17* (6), 1717-1727.

40. Tang, X.; Li, P.; Zhang, Z.; Zhang, Q.; Guo, J.; Zhang, W., An ultrasensitive gray-imaging-based quantitative immunochromatographic detection method for fumonisin B1 in agricultural products. *Food Control* **2017,** *80*, 333-340.

41. He, T.; Wang, Y.; Li, P.; Zhang, Q.; Lei, J.; Zhang, Z.; Ding, X.; Zhou, H.; Zhang, W., Nanobody-based enzyme immunoassay for aflatoxin in agro-products with high tolerance to cosolvent methanol. *Anal Chem***2014,** *86* (17), 8873-80.

42. Lin, R.; Zhang, H.; Zhao, T.; Cao, C.; Yang, D.; Ma, J., Investigation of Au@Pt/C electro-catalysts for oxygen reduction reaction. *Electrochimica Acta* 2012, 62, 263-268.

43. Senthil Kumar, S.; Phani, K. L. N., Exploration of unalloyed bimetallic Au–Pt/C nanoparticles for oxygen reduction reaction. *J Power Sources* 2009, 187 (1), 19-24.

Table of Contents